

Synthesis, Structure, and Activity of Supramolecular Mimics for the Active Site and Arg141 Residue of Copper, Zinc–Superoxide Dismutase

Ying-Hua Zhou,[†] Heng Fu,[†] Wei-Xi Zhao,[†] Wei-Lin Chen,[†] Cheng-Yong Su,[†] Hongzhe Sun,[‡] Liang-Nian Ji,[†] and Zong-Wan Mao^{*†}

MOE Key Laboratory of Bioinorganic and Synthetic Chemistry, School of Chemistry and Chemical Engineering, Sun Yat-Sen University, Guangzhou 510275, China, and Department of Chemistry and Open Laboratory of Chemical Biology, The University of Hong Kong, Pokfulam Road, Hong Kong, China

Received August 15, 2006

Two supramolecular complexes, $[\text{Cu}(\text{L})(\text{H}_2\text{O})_2(\beta\text{-CD})](\text{ClO}_4)_2 \cdot 10.5\text{H}_2\text{O} \cdot \text{CH}_3\text{OH}$ (**1**) and $[\text{Cu}(\text{L})(\text{H}_2\text{O})_2(\beta\text{-GCD})](\text{HClO}_4)(\text{ClO}_4)_2 \cdot 10\text{H}_2\text{O}$ (**2**) ($\text{L} = 4\text{-(4'-tert-butyl-benzyl)diethylenetriamine}$, $\beta\text{-CD} = \beta\text{-cyclodextrin}$, and $\beta\text{-GCD} = \text{mono-6-deoxy-6-guanidinocycloheptaamylose cation}$), have been synthesized. The structure of **1** has been characterized by X-ray crystallography. The 4-*tert*-butyl-benzyl of $[\text{Cu}(\text{L})(\text{H}_2\text{O})_2]^{2+}$ moiety in **1** as a guest inserts into the hydrophobic cavity of the $\beta\text{-CD}$ as a host along the primary hydroxyl side. On the basis of the structure data of **1**, complex **2** was modeled, which showed that the distance between the Cu and C atom of the guanidinium is 5.2 Å, comparable to the corresponding distance in bovine erythrocyte Cu, Zn–SOD (5.9 Å) (SOD = superoxide dismutase). Apparent inclusion stability constants of the host and the guest were measured to be $0.66 (\pm 0.01) \times 10^4$ and $1.15 (\pm 0.03) \times 10^4 \text{ M}^{-1}$ for **1** and **2** respectively. The electronic absorption bands and electronic reflection bands of each complex are almost the same, indicating an identical structure of the complex in aqueous solution and in solid state. The two complexes showed quasi-reversible one-electron Cu(II)/Cu(I) redox waves with redox potentials of -0.345 and -0.338 V for **1** and **2**, respectively. Their SOD-like activities (IC_{50}) were measured to be 0.30 ± 0.01 and $0.17 \pm 0.01 \mu\text{M}$ by xanthine/xanthine oxidase-NBT assay. The enhanced SOD activity of **2** by $\sim 40\%$ compared with **1** suggests that the guanidyl cation in the host of the supramolecular system of **2** can effectively mimic the side chain of Arg141 in the enzyme, which is known to be essential for high SOD activity possibly through steering of the superoxide substrate to and from the active copper ion.

Introduction

Excessive superoxide anion ($\text{O}_2^{\bullet -}$) production leads to oxidative stress and host tissue damage. Copper, zinc-superoxide dismutase (Cu, Zn–SOD) is a ubiquitous enzyme with an essential role in antioxidant defense through catalyzing the dismutation of superoxide anion to oxygen and hydrogen peroxide under physiological conditions.^{1–4} An

imidazolate-bridged copper–zinc binding site, in which the copper ion has a distorted square pyramidal N_4O_w coordination sphere, is absolutely essential for the SOD activity.^{5–7} Recent evidence implicating $\text{O}_2^{\bullet -}$ as a mediator of diseases such as neuronal apoptosis, cancer, and acquired immunodeficiency syndrome, continues to accrue.^{8,9} To further understand structural factors on the origin of the highly efficient superoxide dismutation mechanism, a number of mimics for Cu, Zn–SOD have been reported.^{10–17} The pioneering work provided almost perfect structure models for the active site of Cu, Cu–SOD or Cu, Zn–SOD and

* To whom correspondence should be addressed. Tel: (86) 20-84113788. Fax: (86) 20-84112245. E-mail: csmzw@mail.sysu.edu.cn.

[†] Sun Yat-Sen University.

[‡] The University of Hong Kong.

- (1) (a) Hart, P. J.; Balbirnie, M. M.; Oghara, N. L.; Nersissian, A. M.; Weiss, M. S.; Valentine, J. S.; Eisenberg, D. *Biochemistry* **1999**, *38*, 2167. (b) Ellerby, L. M.; Cabelli, D. E.; Graden, J. A.; Valentine, J. S. *J. Am. Chem. Soc.* **1996**, *118*, 6556.
- (2) Bertini, I.; Banci, L.; Piccioli, M. *Coord. Chem. Rev.* **1990**, *100*, 67.
- (3) Okado-Matsumoto, A.; Fridovich, I. *J. Biol. Chem.* **2001**, *276*, 38388.
- (4) Dupeyrat, F.; Vidaud, C.; Lorphelin, A.; Berthomieu, C. *J. Biol. Chem.* **2004**, *279*, 48091.

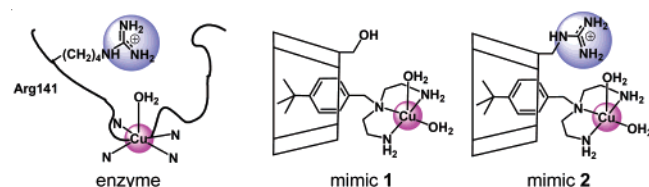
- (5) Tainer, J. A.; Getzoff, E. D.; Richardson, J. S.; Richardson, D. C. *Nature* **1983**, *306*, 284.

- (6) Fridovich, I. *J. Biol. Chem.* **1989**, *264*, 7761.

- (7) McCord, J. M.; Fridovich, I. *J. Biol. Chem.* **1969**, *244*, 6049.

- (8) Thompson, C. B. *Science* **1995**, *267*, 1456.

- (9) Valentine, J. S.; Hart, P. J. *Proc. Natl. Acad. Sci. U.S.A.* **2003**, *100*, 3617.

Scheme 1. Schematic View of Cu, Zn-SOD Active Site with Arg141 Residue and the Two Mimics

offered great efforts, such as a magnetic exchange approach between Cu(II) ions through imidazolate bridge and influenced factors, stability and break modes of imidazolate-bridge in Cu-im-Zn systems, the role of Zn(II) ion by electron effect, and so on. However, the SOD-like activities of almost all mimics were very low. To our knowledge, the highest SOD-like activity (IC_{50}) of reported mimics is only 20% of the bovine erythrocyte Cu, Zn-SOD.^{12c,14}

Many studies on mutants of the enzyme have revealed that several charged residues in Cu, Zn-SOD, such as Arg141 next to the copper(II) ion, promote electrostatic steering of the superoxide substrate to and from copper ion in the active site (Arg141; bovine erythrocyte SOD numbering corresponds to Arg143 for plants and human Cu, Zn-SOD).^{18,19} The X-ray structure of the enzyme shows that a positively charged Arg141 is located in the outer sphere of the active site and is ~ 5.9 Å away from the copper ion (Scheme 1a). Protein engineering has revealed that Arg143 in human Cu, Zn-SOD has mutated to less positive residue Lys, neutral Ile, and negative Glu residues causing 59, 90, and 96% reduction in SOD activity.²⁰ Of reported Cu, Zn-SOD model studies, however, most of them focus on the peculiarity of

the imidazolate bridge, and almost no mimics on the biological function of Arg141 were reported.

Because of the limitations associated with the therapeutic applications of enzymes, such as solution instability, limited cellular accessibility, immunogenicity, bell-shaped dose response curves, short half-lives, costs of production, and proteolytic digestion, a significant amount of research still focuses on SOD mimics with low molecular weights and high activities to understand these defense mechanisms as well as on the development of potential therapeutic antioxidant compounds.²¹ In order to mimic the active site of Cu, Zn-SOD and the positively charged Arg141 residue, we recently investigated the complexation, structure, and SOD activity of a supramolecular complex constructed by an imidazolated-bridged binuclear Cu(II)–Cu(II) complex and β -cyclodextrin (β -CD).²² The guest molecule showed an enhanced SOD-like activity in the presence of guanidyl-modified β -CD. To further confirm the role of guanidyl-modified β -CD in the supramolecular model, two complexes assembled by its mononuclear Cu(II) moiety with the β -CD or the guanidyl-modified β -CD were prepared and isolated and their structures were characterized by X-ray crystallography and calculated by molecular modeling, respectively. Herein their preparation, structures, properties, and SOD activity are reported.

Results and Discussion

Synthesis. By the mixing of a Cu(II) complex and a CD (or directly mixing a copper salt, the ligand, CDs, and excess $NaClO_4$) in aqueous solution at pH ~ 7 , the supramolecular complexes were assembled with a moderate yield. The resulting complex **2** is very soluble in aqueous solution, and thus it can be only isolated with the solvent-evaporation method.

Crystal Structure of $[Cu(L)(H_2O)_2(\beta\text{-CD})](ClO_4)_2 \cdot 10.5H_2O \cdot CH_3OH$ (1**).** The structure of **1** is illustrated in Figure 1, and the selected bond lengths and bond angles are given in Table 2. Complex **1** consists of a supramolecular unit, perchlorate anions, and water molecules. The supramolecular unit is constructed by β -CD as a host and $[Cu(L)(H_2O)_2]^{2+}$ moiety as a guest. The 4-*tert*-butyl-benzyl group of the guest directly inserts into the hydrophobic cavity of the host along the primary hydroxyl side to form $[Cu(L)(H_2O)_2(\beta\text{-CD})]^{2+}$ through hydrophobic interactions. Two β -CD molecules form a head-to-head dimer through H-bond interactions of secondary hydroxyl groups with bond distances of 2.7–3.0 Å. The copper(II) atom in the guest exhibits a distorted square pyramid configuration. The degree of distortion (τ) between trigonal bipyramid to square

- (10) (a) Kolks, G.; Frihart, C. R.; Rabinowitz, H. N.; Lippard, S. J. *J. Am. Chem. Soc.* **1976**, *98*, 5720. (b) O'Young, C.-L.; Dewan, J. C.; Lilienthal, H. R.; Lippard, S. J. *J. Am. Chem. Soc.* **1978**, *100*, 7291. (c) Coughlin, P. K.; Dewan, J. C.; Lippard, S. J.; Watanabe, E.; Lehn, J.-M. *J. Am. Chem. Soc.* **1979**, *101*, 265. (d) Davis, W. M.; Dewan, J. C.; Lippard, S. J. *Inorg. Chem.* **1981**, *20*, 2933. (e) Kolks, G.; Lippard, S. J.; Waszczak, J. V.; Lilienthal, H. R. *J. Am. Chem. Soc.* **1982**, *104*, 717. (f) Strotkamp, K. G.; Lippard, S. J. *Acc. Chem. Res.* **1982**, *15*, 318.
- (11) Lu, Q.; Luo, Q. H.; Dai, A. B.; Zhou, Z. Y.; Hu, G. Z. *J. Chem. Soc., Chem. Commun.* **1990**, 1429.
- (12) (a) Mao, Z.-W.; Chen, D.; Tang, W.-X.; You, K.-B.; Liu, L. *Polyhedron* **1992**, *11*, 191. (b) Mao, Z.-W.; Chen, M.-Q.; Tan, X.-S.; Liu, J.; Tang, W.-X. *Inorg. Chem.* **1995**, *34*, 2889. (c) Li, D.-F.; Li, S.; Yang, D.-X.; Yu, J.-H. Huang, J.; Li, Y.-Z.; Tang, W.-X. *Inorg. Chem.* **2003**, *42*, 6071.
- (13) Pierre, J.-L.; Chautemps, P.; Refaif, S.; Beguin, C.; Marzouki, A. E.; Serratrice, G.; Saint-Aman, E.; Rey, P. J. *Am. Chem. Soc.* **1995**, *117*, 1965.
- (14) Ohtsu, H.; Shimazaki, Y.; Odani, A.; Yamauchi, O.; Mori, W.; Itoh, S.; Fukuzumi, S. *J. Am. Chem. Soc.* **2000**, *122*, 5733.
- (15) Weser, U.; Schubotz, L. M.; Lengfelder, E. *J. Mol. Catal.* **1981**, *13*, 249.
- (16) (a) Hendricks, H. M. J.; Birker, P. J. W. L.; Verschoor, G. C.; Reedijk, J. *J. Chem. Soc., Dalton Trans.* **1982**, 623. (b) Tabbi, G.; Driessen, W. L.; Reedijk, J.; Bonomo, R. P.; Veldman, N.; Spek, A. L. *Inorg. Chem.* **1997**, *36*, 1168.
- (17) Jitsukawa, K.; Harata, M.; Arai, H.; Sakurai, H.; Masuda, H. *Inorg. Chim. Acta* **2001**, *324*, 108.
- (18) (a) Getzoff, E. D.; Tainer, J. A.; Weiner, P. K.; Kollman, P. A.; Richardson, J. S.; Richardson, D. C. *Nature* **1983**, *306*, 287. (b) Fisher, C. L.; Cabelli, D. E.; Hallewell, R. A.; Beroza, P. Lo, T. P.; Getzoff, E. D.; Tainer, J. A. *Proteins: Struct., Funct., and Genet.* **1997**, *29*, 103. (c) Cudd, A.; Fridovich, I. *J. Biol. Chem.* **1982**, *257*, 11443. (d) Cudd, A.; Fridovich, I. *FEBS Lett.* **1982**, *144*, 181.
- (19) (a) Beyer, W. F.; Fridovich, I.; Mullenbach, G. T.; Hallewell, R. A. *J. Biol. Chem.* **1987**, *263*, 11182. (b) Banci, L.; Bertini, I.; Luchinat, C.; Hallewell, R. A. *J. Am. Chem. Soc.* **1988**, *110*, 3629.

- (20) (a) Banci, L.; Carloni, P.; Penna, G. L.; Orioli, P. L. *J. Am. Chem. Soc.* **1992**, *114*, 6994. (b) Banci, L.; Bertini, I.; Bauer, J. D.; Hallewell, R. A.; Viezzoli, M. S. *Biochemistry* **1993**, *32*, 4384. (c) Banci, L.; Bertini, I.; Bertini, Del Conte, R.; Viezzoli, M. S. *Biospectroscopy* **1999**, *5*, S33.
- (21) Salvemini, D.; Wang, Z. Q.; Zweier, J. L.; Samouilov, A.; Macarthur, H.; Misko, T. P.; Currie, M. G.; Cuzzocrea, S.; Sikorski, J. A.; Riley, D. P. *Science* **1999**, *286*, 304.
- (22) Fu, H.; Zhou, Y. H.; Chen, W. L.; Deging, Z. G.; Tong, M. L.; Ji, L. N.; Mao, Z. W. *J. Am. Chem. Soc.* **2006**, *128*, 4924.

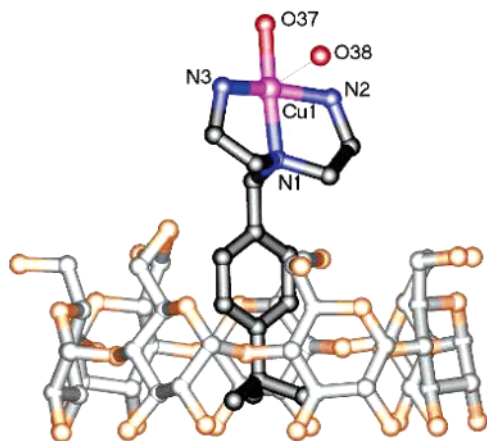


Figure 1. The supramolecular molecular structure of $[\text{Cu}(\text{L})(\text{H}_2\text{O})-(\beta\text{CD})]^{2+}$ in **1**.

Table 1. Crystallographic Data for **1**

complex	$[\text{Cu}(\text{L})(\text{H}_2\text{O})(\text{ClO}_4)_2(\beta\text{CD})]$
empirical formula	$\text{C}_{58}\text{H}_{126}\text{Cl}_2\text{N}_3\text{O}_{56.5}\text{Cu}$
fw	1904.06
T , K	173(2)
wavelength, Å	0.71073
crys syst	orthorhombic
space group	$C222_1$
a , Å	19.416(2)
b , Å	23.882(2)
c , Å	37.771(3)
V , Å ³	17 515(2)
Z	8
D_{calcd} , g cm ⁻³	1.444
μ , mm ⁻¹	0.419
independent reflns	15 521
GOF on F^2	1.017
R_1/R_2 (obsd data)	0.0730/0.1931 ^a

$$^a w = 1/[s^2F_o^2 + (0.1354P)^2 + 42.2768P]. P = (F_o^2 + 2F_c^2)/3.$$

Table 2. Selected Bond Lengths (Å) and Angles (deg) for Metal Environment of **1** Determined by X-ray Analysis

Cu(1)–N(1)	2.143(3)	Cu(1')–N(1)	1.952(3)
Cu(1)–N(2)	2.046(4)	Cu(1')–N(2')	2.035(6)
Cu(1)–N(3)	1.992(3)	Cu(1')–N(3')	2.014(7)
Cu(1)–O(37)	1.962(3)	Cu(1')–O(37')	1.982(7)
Cu(1)–O(38)	2.649(4)	Cu(1')–O(38')	2.426(8)
Cu(1')–N(1)–Cu(1)	25.56(6)	O(37)–Cu(1)–N(3)	95.49(1)
O(37)–Cu(1)–N(2)	95.75(1)	N(3)–Cu(1)–N(2)	157.68(2)
O(37)–Cu(1)–N(1)	176.83(1)	N(3)–Cu(1)–N(1)	87.56(1)
N(1)–Cu(1')–N(2')	90.6(2)	O(37')–Cu(1')–N(2')	93.3(3)
N(3')–Cu(1')–N(2')	164.5(4)	N(1)–Cu(1')–O(38')	98.3(3)
N(2)–Cu(1)–N(1)	81.09(1)	O(37)–Cu(1)–O(38)	80.79(1)
N(1)–Cu(1)–O(38)	98.81(1)	N(1)–Cu(1')–O(37')	173.1(3)
N(1)–Cu(1')–N(3')	81.3(2)	O(37')–Cu(1')–N(3')	96.2(3)
O(37')–Cu(1')–O(38')	88.1(3)	N(3')–Cu(1')–O(38')	90.0(4)
N(3)–Cu(1)–O(38)	82.10(1)	N(2)–Cu(1)–O(38)	80.75(2)
N(2')–Cu(1')–O(38')	78.0(3)		

pyramid can be estimated according to a previous report.²³ For an ideal square pyramidal geometry, τ is equal to zero, whereas it becomes unity for an ideal trigonal bipyramidal geometry. The calculated τ -value of 0.32 indicates that the geometry of coordination around the Cu atom is slightly closer to a square pyramidal configuration.

Molecular Modeling of $[\text{Cu}(\text{L})(\text{H}_2\text{O})_2(\beta\text{-GCD})](\text{HClO}_4)(\text{ClO}_4)_2 \cdot 10\text{H}_2\text{O}$ (2**).** To find a potential correlation

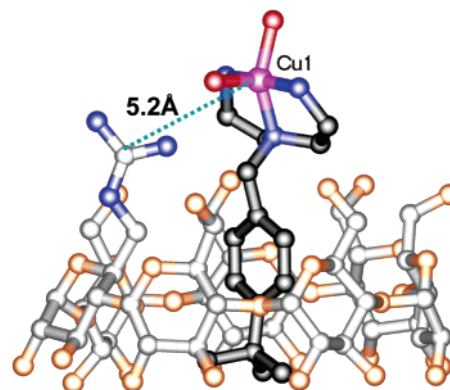


Figure 2. Molecular modeling of **2** calculated by the PM3 method.

between structure and reactivity of guanidinium-containing **2**, semiempirical calculation for **2** was performed using the PM3 method (Figure 2). The result showed that the distance between Cu atom in the guest and central C atom of the guanidinium in the host is around 5.2 Å, comparable to the corresponding distance in bovine erythrocyte SOD (5.88 Å). In the designed supramolecular system, therefore, the guanidinium of the CD molecule is located within the effective range around the Cu(II) center and can serve as a mimic for Arg141 in the enzyme.

Electronic Spectra. The electronic reflection and absorption spectra of two complexes in solid or in aqueous solution were characterized, with broad peaks centered in the range of 619–622 nm. Almost the same reflection and absorbance bands indicated that each N_3O_2 chromosphere around the Cu(II) ion keeps the same configuration and is not changed by the modified groups on the host or solvent molecules. This absorbance can be attributed to $d \rightarrow d^*$ transitions involving Cu(II) ions bound to a distorted square pyramid. Previously, absorbance bands in the range of 630–680 nm were observed for wild type Cu, Zn–SODs.²⁴ Therefore, the electronic structure of the Cu(II) center in two mimics was similar to that of the Cu(II) center in Cu, Zn–SOD.

Stability Constant of the Inclusion Complex. To further understand the guest–host inclusion complexation, the stability constants of the inclusion complexes were determined by following the changes of absorbance at 262 nm by electronic absorption spectroscopy. Cu(II) with L complex was titrated with various concentrations of $\beta\text{-CD}/\beta\text{-GCD}$ according to a previously described method.²⁵ For a cyclodextrin, which is fairly rigid, the guest molecule must fit snugly into the cavity. Since the combined reduction in cavity–water and insert–water surface areas is the driving force for complexation, the most ideal situation for complexation is a snug fit of the nonpolar portion of the guest molecule into the nonpolar cyclodextrin cavity.¹⁴ This would remove a maximum amount of water molecules from the cavity and from the molecule surface. The stability constants

(24) Battistoni, A.; Pacello, F.; Mazzetti, A. P.; Capo, C.; Kroll, J. S.; Langford, P. R.; Sansone, A.; Donnarumma, G.; Valenti, P.; Rotilio, G. *J. Biol. Chem.* **2001**, 276, 30315.

(25) (a) Chen, Y.; Xiang, P.; Li, G.; Chen, H.-L.; Chinnakali, K.; Fun, H.-K. *Supramol. Chem.* **2002**, 14, 339. (b) Itoh, T.; Hisada, H.; Usui, Y.; Fujii, Y. *Inorg. Chim. Acta* **1998**, 283, 51.

(23) Addison, A. W.; Rao, T. N. *J. Chem. Soc., Dalton Trans.* **1984**, 1349.

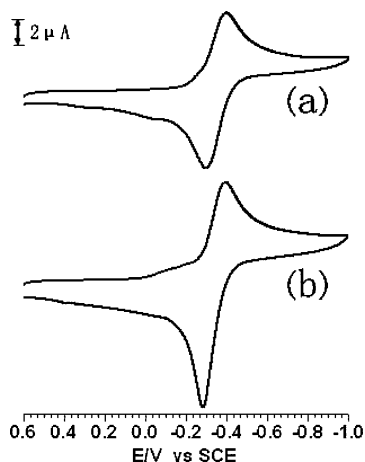


Figure 3. Cyclic voltammograms of (a) **1** and (b) **2** (1 mM) in H₂O containing 0.1 M NaClO₄; working electrode, glassy carbon; counter electrode, Pt wire; reference electrode, SCE electrode; scan rate, 50 mV s⁻¹.

Table 3. Comparison of Chemical Properties and SOD-like Activities of **1** and **2**

property	1	2
K_{sc}	$6.6 (\pm 0.03) \times 10^3$	$1.15 (\pm 0.03) \times 10^4$
abs max (solid) (nm)	619	619
abs max (H ₂ O) (nm)/ ϵ (M ⁻¹ cm ⁻¹)	621(83)	622(113)
Cu(II)/Cu(I) potential vs SCE (V)	-0.345	-0.338
IC ₅₀	0.30 ± 0.01	0.17 ± 0.01
k_{cat} (M ⁻¹ s ⁻¹)	9.90×10^7	1.75×10^8

(K_{sc}) were calculated to be $6.64 (\pm 0.03) \times 10^3$ and $1.15 (\pm 0.03) \times 10^4$ M⁻¹ for **1** and **2**, respectively. In complex **2**, the H-bonding between guanidinium on the host and the ligands of the guest may account for its higher stability constant.

Electrochemistry. The electrochemical properties of mimics were studied by cyclic voltammetry.^{12c} Cyclic voltammograms were collected in degassed aqueous solution (Figure 3). Both complexes showed complete reversible one-electron redox waves with redox potentials of -0.345 and -0.338 V for **1** and **2**, respectively (see Table 3). The potentials can be assigned to the Cu(II)/Cu(I) redox couple. It is known that an adequate Cu(II)/Cu(I) redox potential for effective catalysis of superoxide radical must be required between E° -0.405 V vs SCE for O₂/O₂⁻ and E° 0.645 V vs SCE for O₂⁻/H₂O₂.^{12c} In the determined range, no cyclic voltammograms of CDs and L were observed.

SOD-like Activity. The SOD-like activities of mimics were examined by xanthine/xanthine oxidase-NBT assay and are shown in Figure 4.^{16,26,27} The IC₅₀ values are listed in Table 3, including corresponding second-order rate constants calculated according to $k_{cat} = k_{NBT}[NBT]/IC_{50}$, where $k_{NBT} = 5.94 \times 10^4$ M⁻¹ s⁻¹.²⁴ The activity of bovine erythrocyte SOD was also measured for comparison with the IC₅₀ value of 0.042 ± 0.01 μM, being almost identical to that (0.04 μM) reported previously.¹⁵ Neither the ligand nor the CDs

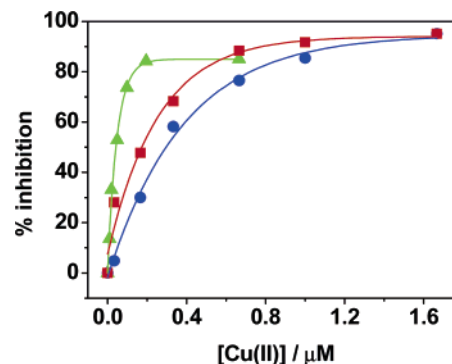


Figure 4. Percentage of inhibition of superoxide radicals formed by xanthine/xanthine oxidase enzyme assayed by NBT⁺ absorption at 560 nm in the presence of bovine erythrocyte SOD (▲), **1** (■), and **2** (●) (500 μM xanthine, 0.04 unit of xanthine oxidase and 500 μM NBT, 0.1 M phosphate buffer, pH = 7.8).

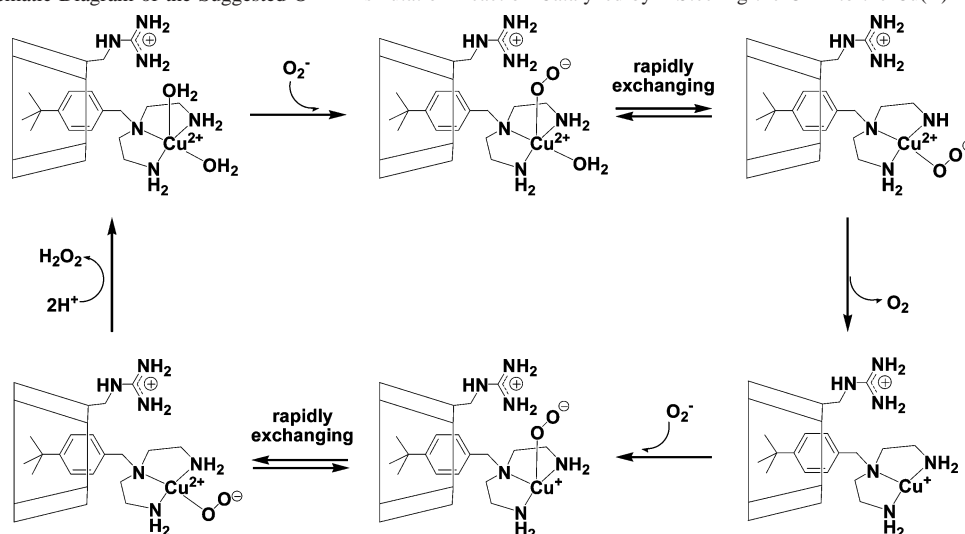
exhibited any O₂⁻ scavenger effects under the same conditions. It can be seen from Table 3 that only a moderate SOD-like activity was observed for **1** due to the lack of positive charge around the Cu(II) ion. The activity of **2** with positive charge around the Cu(II) ion exhibited a slightly higher SOD-like activity (IC₅₀ = 0.17 ± 0.01 μM) than those of the best SOD mimics reported in the literature,^{12c} which is also comparable to its dinuclear analogues.²² The introduction of a guanidinium in **2** enhanced SOD-like activity by ~40% in comparison with **1** which has a lack of guanidinium.

Recently, we reported two supramolecular systems constructed by an imidazolate-bridged Cu(II)-Cu(II) complex and unmodified β-CD/guanidyl-modified β-CD.²² In the unmodified β-CD complexation system, **1** has slightly lower SOD activity than its corresponding dinuclear system (IC₅₀ = 0.23 μM). In the guanidyl-modified β-CD complexation system, **2** has almost the same SOD activity as the corresponding dinuclear system (IC₅₀ = 0.20–0.16 μM). This indicates that the guanidyl cation plays a more important role than the imidazolate bridge for SOD activity in model compounds. In the enzyme, the imidazolate bridge can stabilize the space structure of the protein and provide needed protons to the peroxide anion during the catalytic cycle. Since the proton exchange between substrates and buffer is a rapid process in the small model systems, the buffer can directly transfer protons to peroxide anion in the mechanism.

Our result strongly supported the conclusion that the Arg141 in the enzyme is indeed essential for high-SOD activity and can steer the superoxide substrate to and from the active copper ion. On the basis of our results and previously suggested catalytic mechanisms,^{1,2} a possible mechanism steering the O₂⁻ to the Cu(II) for the catalytic process is proposed (Scheme 2). First, a superoxide anion is attracted by the Cu(II) ion under the orienting influence of the guanidyl cation. Second, the superoxide anion binding directly to the Cu(II) ion can exchange rapidly between the axial and the planar position of distorted square pyramid,^{1a} leading it to give up its electron and form an O₂ molecule. Third, the electrically neutral oxygen molecule leaves. Fourth, a second superoxide anion is attracted by the Cu(I) ion still under the orienting influence of the guanidyl cation.

(26) Beauchamp, C.; Fridovich, I. *Anal. Biochem.* **1971**, *44*, 276.

(27) Schepetkin, I.; Potapov, A.; Khlebnikov, A.; Korotkova, E.; Lukina, A.; Malovichko, G.; Kirpotina, L.; Quinn, M. T. *J. Biol. Inorg. Chem.* **2006**, *11*, 499.

Scheme 2. A Schematic Diagram of the Suggested $\text{O}_2^{\cdot -}$ Dismutation Reaction Catalyzed by **2** Steering the $\text{O}_2^{\cdot -}$ to the Cu(II)^a 

^a All coordinated water molecules are omitted for clarity.

Fifth, the superoxide anion binds again to the Cu(I) ion to accept an electron and a proton from the buffer. Since the proton exchange between the substrates and buffer is a rapid process, the superoxide anion further combines another proton from the solution to form a H_2O_2 molecule. Finally, electrically neutral hydrogen peroxide leaves, completing a catalytic cycle.

Conclusion

The mimic with guanidyl cation exhibits a potent SOD activity. A guanidyl cation located in the effective range around the Cu(II) ion is crucial for attracting the superoxide anion to and from the active copper ion and may play a role of Arg141 in the Cu,Zn-SOD . The general strategy in this report may be extended to the design of models of other metalloenzymes.

Experimental Section

Materials. Bovine erythrocyte SOD, xanthine oxidase, β -cyclodextrin, and other special reagents were purchased from Aldrich-Sigma Chemical Company. Xanthine and nitro-blue tetrazolium (NBT) were purchased from BBI. Organic reagents were reagent grade and redistilled before use. Water used in all physical measurement experiments was Milli-Q grade. Ligand and β -GCD cation were prepared as described and were confirmed by element analysis.^{22,28}

$[\text{Cu(L)(H}_2\text{O)}_2(\beta\text{-CD})](\text{ClO}_4)_2 \cdot 10.5\text{H}_2\text{O} \cdot \text{CH}_3\text{OH}$ (1**).** To an aqueous solution of $\text{Cu}(\text{ClO}_4)_2 \cdot 6\text{H}_2\text{O}$ (0.185 g, 0.5 mmol) was added the aqueous solution (5 mL) of $\text{L} \cdot 3\text{HCl}$ (0.188 g, 0.5 mmol) dropwise under constant stirring. And then β -CD (0.567 g, 0.5 mmol) was added, followed by the adjustment of the pH to ca. 7. After the solution was stirred for 30 min and filtered, the solution was placed in a desiccator with P_2O_5 for slow evaporation. Several days later, blue cubic crystals suitable for X-ray analysis were obtained with 46% yield. Anal. Calcd for $\text{C}_{58}\text{H}_{126}\text{N}_6\text{O}_{56.5}\text{Cl}_2\text{Cu}$: C, 36.75; H, 6.55; N, 2.26. Found: C, 36.40; H, 6.78; N, 1.85.

$[\text{Cu(L)(H}_2\text{O)}_2(\beta\text{-GCD})](\text{ClO}_4)_3 \cdot 10\text{H}_2\text{O}$ (2**).** The complex **2** was prepared similarly to **1** except that (β -GCD) ClO_4 (0.638 g, 0.5 mmol)

was used instead of β -CD. After filtration, the solution was kept at 40 °C by water bath. Several days later, blue powders were obtained with 86% yield. Anal. Calcd for $\text{C}_{58}\text{H}_{121}\text{N}_6\text{Cl}_3\text{O}_{56}\text{Cu}$: C, 35.39; H, 6.20; N, 4.27. Found: C, 35.26; H, 6.287; N, 4.398.

Caution: Perchlorate salts of organic compounds are potentially explosive; these compounds must be prepared and handled with great care!

Physical Measurements. Elemental contents were analyzed by a Perkin-Elmer 240 elemental analyzer. Cyclic voltammetrical measurements were carried out on a CHI 600C electrochemical analyzer. The SOD activity was measured at 560 nm with a Varian 300 spectrophotometer with a temperature controller.

X-ray Crystallography. Single-crystal X-ray data of **1** was collected on a Bruker Smart Apex CCD diffractometer at 173 K, both with graphite-monochromated $\text{Mo K}\alpha$ radiation ($\lambda = 0.71073$ Å). The reflections were corrected for Lorentz and polarization effects, and empirical absorption corrections were applied using the SADABS program.²⁹ The space groups were determined from systematic absences and confirmed by the results of refinement. The structure of **1** was solved by direct methods using the SHELXTL software suite and Sir2004.^{30,31} All non-hydrogen atoms were refined with anisotropic displacement parameters except some of the badly disordered ones. All H atoms of the organic ligands were placed at idealized positions and refined as riding atoms. Almost all atoms of the host β -CD molecule were normal, but a few atoms of the guest molecule exhibited serious disorder. In addition, perchlorate anions are severely disordered. Such disorder situations often appear in guest–host inclusion complexes of cyclodextrins,³² always resulting in some abnormal bond lengths and angles. The structural refinements were carried out with a few restraints owing to the serious disorder phenomenon; however, not all seemingly abnormal bond distances and angles were modeled

(29) Sheldrick, G. M. *SADABS, Program for Scaling and Correction of Area Detector Data*; University of Göttingen: Göttingen, Germany, 1996.

(30) (a) Sheldrick, G. M. *SHELXS-97, Program for Crystal Structure Solution*; University of Göttingen: Göttingen, Germany, 1997. (b) Sheldrick, G. M.; *SHELXL-97, Program for Crystal Structure Refinement*; University of Göttingen: Göttingen, Germany, 1997.

(31) Burla, M. C.; Calandro, R.; Camalli, M.; Carrozzini, B.; Cascarano, G. L.; Caro, L. De; Giacovazzo, C.; Polidori, G.; Spagna, R. *J. Appl. Crystallogr.* **2005**, 38, 381–388.

(28) Schneider, P. W.; Collman, J. P. *Inorg. Chem.* **1968**, 7, 2010.

because they do not affect our general understanding of the host–guest chemistry. Crystallographic data of **1** are listed in Table 1.

Measurement of UV–vis Spectroscopy. With a Varian Cary 100 UV–vis spectrophotometer equipped with a temperature controller (± 0.1 °C), inclusion stability constants were determined by monitoring the changes of UV absorption of 0.1 mM metal complexes solutions in a Tris buffer upon addition of different mol ratios of the β -CD or β -GCD at pH = 7.8, 25 ± 0.1 °C, and 0.1 M NaClO₄.

Electrochemistry. The redox potentials of the complexes were determined by the cyclic voltammetry method using the conventional three-electrode system of glass carbon electrode as the working electrode, platinum wire as the counter electrode, and saturated calomel electrode (SCE) as the reference electrode. The solution of perchlorate sodium (NaClO₄, 0.1 M) was used as supporting electrolyte. The experiments were carried out in aqueous solution of the inclusion complexes (1 mM) under nitrogen atmosphere at room temperature.

SOD Activity. Superoxide anion ($O_2^{\bullet -}$) was generated in enzymatic (xanthine/xanthine oxidase) system in the presence or absence of test compounds, and $O_2^{\bullet -}$ production was determined by monitoring the reduction of NBT to monoformazan dye at 560 nm at 25 ± 0.1 °C.^{26,27} An appropriate amount of xanthine oxidase was added to a mixture of 500 μ M NBT, 500 μ M xanthine, and 0–1.0 μ M complex dissolved in 50 mM phosphate buffer (pH 7.8) to cause a variation of absorbance ($\Delta A_{560}/\Delta t_{\min}$) of 0.025 ± 0.005 .

- (32) (a) Chen, Y.; Xiang, P.; Li, G.; Chen, H.-L.; Chinnakali, K.; Fun, H.-K. *Supramol. Chem.* **2002**, *14*, 339. (b) Navaza, A.; Iroulart, M. G.; Navaza, J. J. *Coord. Chem.* **2000**, *51*, 153. (c) Chen, Y.; Chen, H.-L.; Yang, Q.-C.; Song, X.-Y.; Duan, C.-Y.; Mak, T. C. W. *J. Chem. Soc., Dalton Trans.* **1999**, 629. (d) Luo, L.-B.; Chen, Y.; Chen, H.-L.; Zhang, Z.-Y.; Zhou, Z.-Y.; Mak, T. C. W. *Inorg. Chem.* **1998**, *37*, 6147. (e) Klingert, B.; Rihs, G. *J. Chem. Soc., Dalton Trans.* **1991**, 2749. (f) Alston, D. R.; Slawin, A. M. Z.; Stoddart, J. F.; Williams, D. J.; Zarzycki, R. *Angew. Chem., Int. Ed. Engl.* **1988**, *27*, 1184. (g) Alston, D. R.; Slawin, A. M. Z.; Stoddart, J. F.; Williams, D. J. *Chem. Commun.* **1985**, 1602.

The percentage inhibition (% *I*) of NBT⁺ formation was calculated from equation: (% *I*) = $(A_0 - A_s)/A_0 \times 100$, in which *A*₀ and *A*_s are the maximum absorbance values due to NBT⁺ at 560 nm in the absence and in the presence of the inclusion complex. By plotting the % *I* as a function of complex concentration, the IC₅₀ values were calculated.

Molecular Modeling. Semiempirical calculation for **2** was performed using the PM3 method. The molecular structures were generated with the molecular builder supplied in the Spartan 04 package and optimized in Gaussian 03.³³ Selected bond distances for **2** are listed in Table S1.

Acknowledgment. Supported by the NSFC (20231010, 20529101) and NSFCD (04009703). We thank Prof. Xiao-Ming Chen for his help with X-ray crystallography.

Supporting Information Available: Spectral and CIF data. This material is available free of charge via the Internet at <http://pubs.acs.org>.

IC061541D

- (33) Frisch, M. J.; Trucks, G. W.; Schlegel, H. B.; Scuseria, G. E.; Robb, M. A.; Cheeseman, J. R.; Montgomery, J. A., Jr.; Vreven, T.; Kudin, K. N.; Burant, J. C.; Millam, J. M.; Iyengar, S. S.; Tomasi, J.; Barone, V.; Mennucci, B.; Cossi, M.; Scalmani, G.; Rega, N.; Petersson, G. A.; Nakatsuji, H.; Hada, M.; Ehara, M.; Toyota, K.; Fukuda, R.; Hasegawa, J.; Ishida, M.; Nakajima, T.; Honda, Y.; Kitao, O.; Nakai, H.; Klene, M.; Li, X.; Knox, J. E.; Hratchian, H. P.; Cross, J. B.; Adamo, C.; Jaramillo, J.; Gomperts, R.; Stratmann, R. E.; Yazyev, O.; Austin, A. J.; Cammi, R.; Pomelli, C.; Ochterski, J. W.; Ayala, P. Y.; Morokuma, K.; Voth, G. A.; Salvador, P.; Dannenberg, J. J.; Zakrzewski, V. G.; Dapprich, S.; Daniels, A. D.; Strain, M. C.; Farkas, O.; Malick, D. K.; Rabuck, A. D.; Raghavachari, K.; Foresman, J. B.; Ortiz, J. V.; Cui, Q.; Baboul, A. G.; Clifford, S.; Cioslowski, J.; Stefanov, B. B.; Liu, G.; Liashenko, A.; Piskorz, P.; Komaromi, I.; Martin, R. L.; Fox, D. J.; Keith, T.; Al-Laham, M. A.; Peng, C. Y.; Nanayakkara, A.; Challacombe, M.; Gill, P. M. W.; Johnson, B.; Chen, W.; Wong, M. W.; Gonzalez, C.; Pople, J. A. *Gaussian 03, Revision B.03*; Gaussian, Inc.: Pittsburgh, PA, 2003.